

Taylor & Francis
Taylor & Francis Group

Journal of Enzyme Inhibition and Medicinal Chemistry

ISSN: 1475-6366 (Print) 1475-6374 (Online) Journal homepage: https://www.tandfonline.com/loi/ienz20

Inhibition of mammalian carbonic anhydrases I-XIV with grayanotoxin III: solution and in silico studies

Serdar Durdagi, Gabriele Scozzafava, Daniela Vullo, Hüseyin Sahin, Sevgi Kolayli & Claudiu T. Supuran

To cite this article: Serdar Durdagi, Gabriele Scozzafava, Daniela Vullo, Hüseyin Sahin, Sevgi Kolayli & Claudiu T. Supuran (2014) Inhibition of mammalian carbonic anhydrases I-XIV with grayanotoxin III: solution and in silico studies, Journal of Enzyme Inhibition and Medicinal Chemistry, 29:4, 469-475, DOI: 10.3109/14756366.2013.804072

To link to this article: https://doi.org/10.3109/14756366.2013.804072

Published online: 05 Aug 2013.

Submit your article to this journal

Article views: 528

View related articles

View Crossmark data

Citing articles: 27 View citing articles

Full Terms & Conditions of access and use can be found at
https://www.tandfonline.com/action/journalInformation?journalCode=ienz20

Journal of Enzyme Inhibition and Medicinal Chemistry

http://informahealthcare.com/enz
ISSN: 1475-6366 (print), 1475-6374 (electronic)

J Enzyme Inhib Med Chem, 2014; 29(4): 469–475
© 2014 Informa UK Ltd. DOI: 10.3109/14756366.2013.804072

informa healthcare

ORIGINAL ARTICLE

Inhibition of mammalian carbonic anhydrases I-XIV with grayanotoxin III: solution and in silico studies

Serdar Durdagi[1,2], Gabriele Scozzafava[3], Daniela Vullo[4], Hüseyin Sahin[5], Sevgi Kolayli[5], and Claudiu T. Supuran[4,6]

[1]University of Calgary, Institute for Biocomplexity and Informatics, Calgary, AB, Canada, [2]Bahcesehir University, Faculty of Medicine, Department of Biophysics, Istanbul, Turkey, [3]University of Florence, Dipartimento di Economia, Ingegneria, Scienze e Tecnologie Agrarie e Forestali, Florence, Italy, [4]Università degli Studi di Firenze, Polo Scientifico, Laboratorio di Chimica Bioinorganica, Rm. 188, Via della Lastruccia 3, Sesto Fiorentino, Florence, Italy, [5]Department of Chemistry, Faculty of Sciences, Karadeniz Technical University, Trabzon, Turkey, and [6]University of Florence, Neurofarba Department, Sezione di Scienze Farmaceutiche, Via Ugo Schiff 6, 50019 Sesto Fiorentino, Florence, Italy

Abstract

Grayanotoxin III (GTX3) was investigated for inhibition of all catalytically active mammalian carbonic anhydrase (CA, EC 4.2.1.1) isoforms, i.e. CA I to CA XIV. It showed micromolar inhibition (K_Is of 8.01 and 6.13 μM) for cytosolic isoforms CA I and II, respectively. GTX3 showed a submicromolar inhibition (K_Is in the range of 0.51–2.15 μM) for the remaining cytosolic (CA III, VII and XIII), membrane-associated/transmembrane (CA IV, IX, XII and XIV), mitochondrial (CA VA and CA VB) and secreted (CA VI) isoforms. This inhibition profile is very different from that of the sulfonamide CA inhibitors (CAIs), which possess different clinical applications. A molecular docking study for GTX3 within the active sites of CA I and II assisted to the understanding of molecular mechanism of the ligand. The interesting inhibition profile, coupled with various possibilities of interacting with the enzyme active site make this family of natural compounds attractive leads for designing novel chemotypes acting as CAIs.

Keywords

Carbonic anhydrase, grayanotoxin III, molecular docking

History

Received 17 April 2013
Accepted 7 May 2013
Published online 31 July 2013

Introduction

Grayanotoxins (GTXs) are tetracyclic diterpenoid compounds found in many plants belonging to the Ericaceae family and are poisonous to mammals[1–4]. The most investigated grayanotoxin intoxications involves eating the so-called ''*mad honey*'', i.e. honey contaminated by *Rhododendron spp.* nectar[3]. This is one of the common food intoxications encountered in humans and livestock in Turkey and Japan[2,3]. GTX intoxication symptoms include dizziness, weakness, excessive perspiration, hypersalivation, nausea, vomiting and paresthesias[3]. The severe intoxication may lead to life-threatening cardiac complications such as complete atrioventricular block, due to a specific increase in resting sodium permeability as well as activation of voltage-sensitive sodium channels[3,5]. Possible involvement of muscarinic cholinergic neurons in the GTX-III-induced salivation were also suggested[5]. Recently, honey extracts from the endemic plant in the Black Sea region *Rhododendron ponticum*, were investigated for their inhibitory effects against the metalloenzyme carbonic anhydrase (CA, EC 4.2.1.1), more precisely the human (h) isoforms hCA I and II, by our groups[6]. We have hypothesized that these enzyme inhibitory effects may be due to the presence of GTXs (and more specifically, GTX III, abbreviated here as GTX3) in the mad honey samples, since honey from other types of flower than *R. ponticum* were devoid of such properties[6].

The CAs are widespread metalloenzymes found in organisms all over the tree of life, including vertebrates[7–10]. In such organisms, 16 isozymes have been characterized to date, many of which are involved in critical physiological processes. They catalyze the following reaction[7–11]: $CO_2 + H_2O \leftrightarrow H^+ + HCO_3^-$. In humans, CAs are present in a large variety of tissues including the gastrointestinal tract, the reproductive tract, the nervous system, kidneys, lungs, skin and eyes[10]. The different isozymes are localized in different parts of the cell with CA I and CA II, important isozymes in normal cells, being localized in the cytosol[10]. Many of the CA isozymes are important therapeutic targets with the potential to be inhibited to treat a range of disorders[7–12]. CA II plays a role in bicarbonate production in the eye and is, therefore, a target for therapy of eye disease such as glaucoma[7]. Indeed, CA inhibitors (CAIs) of the sulfonamide type such as dorzolamide DZA or brinzolamide BRZ are topically used antiglaucoma agents[7–10], whereas the older drugs, such as acetazolamide AAZ or dichlorophenamide DCP show the same action through systemic administration, which however leads to a wide range of side effects due to inhibition of the enzyme from other organs than the target one, i.e. the eye[7] (Scheme 1)[11–15]. CA IX and CA XII, are transmembrane isoforms with an extracellular active site, which were shown to be overexpressed in many types of tumors.

As some solid tumors grow in cancer patients, hypoxic regions are formed, particularly in the interior of the tumor[13]. The gene expression profile of a hypoxic cancer cell is different from that of other cancer cells in a normally-oxygenated environment,

Address for correspondence: Serdar Durdagi, Max Planck Institute for Dynamics of Complex Technical Systems, Magdeburg, Germany. Tel: +49-391-6110-284. Fax: +49-391-6110-500. E-mail: durdagi@mpi-magdeburg.mpg.de

Claudiu T. Supuran, Università degli Studi di Firenze, Polo Scientifico, Laboratorio di Chimica Bioinorganica, Rm. 188, Via della Lastruccia 3, 50019 Sesto Fiorentino, Florence, Italy. Tel: +39-055-457 3005. Fax: +39-055-4573385. E-mail: claudiu.supuran@unifi.it

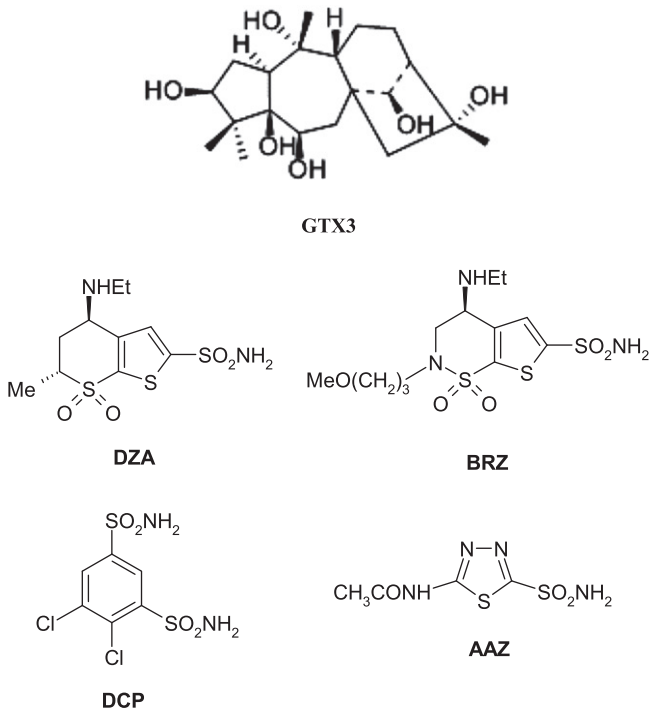

Scheme 1. 2D molecular structures of GTX3, DZA, BRZ, DCP, and AAZ.

i.e. in normoxic conditions[11–15]. Under hypoxia, the distribution of CA isoforms is altered as compared with normoxic cells[11–14]. CA IX and CA XII are both extracellularly localized on hypoxic tumor cells[13–15]. These enzymes play various roles in tumorigenesis, by regulating pH inside and outside the tumor cells[11], interfering with phosphorylation of various proteins or by playing a role in the cell-cell adhesion[11–15]. They therefore provide a target for cancer therapy because they are relatively specific to the hypoxic tumor cells and appear to be important in their survival and proliferation[11]. Indeed, several antibodies targeting CA IX are in Phase III clinical development for the treatment of solid tumors (or for their imaging) whereas some small molecule inhibitors are also in advanced preclinical evaluation[16,17].

The classical CA inhibitors (CAIs) are the sulfonamides and their isosteres (sulfamates, sulfamides, etc)[7,17,18]. However, most of these compounds non-selectively inhibit many of the 16 CA isoforms known to date in mammals[7–11]. Thus, efforts have been made to find different CAIs, from the sulfonamide, sulfamate and sulfamide ones. Indeed, recently the coumarins[19] were discovered as mechanism-based inhibitors which act as prodrugs and bind in a very different mode compared to sulfonamides and their isosteres[20], whereas some polyamines (such as spermine)[21], as well as a range of natural product phenols[22,23] were also investigated and showed interesting such properties and novel mechanisms of inhibition. Following our preliminary communication[6] on the effects of mad honey against CA I and II, we report here an inhibition study of all catalytically active mammalian CA isoforms (i.e. CA I–CA XIV) with GTX3. As we were unable to obtain high-quality crystals of the CA–GTX3 adducts (for X-ray crystallography), we also performed a molecular docking study for the GTX3 within the active sites of isoforms CA I and II, in order to understand the underlying inhibition mechanism of the compound against CAs.

Results and discussion

Pure GTX3 has been investigated for the inhibition of all human (h) CA isoforms possessing catalytic activity, i.e. hCA I–hCA XIV. Indeed, three isoforms (hCA VIII, X and XI) are devoid of catalytic activity as they miss one or more of the histidine residues coordinating the catalytically crucial Zn(II) ion from the enzyme active site[7–10]. We used a stopped-flow, CO_2 hydrase assay for measuring CA activity and inhibition[24].

Table 1. Inhibition data of mammalian isoforms hCA I-XIV with grayanotoxin III, and the sulfonamide inhibitor dichlorophenamide DCP (as standard) by a stopped-flow CO_2 hydrase assay[24].

	K_I (μM)*	
Compound/Isoform	GTX3	DCP
hCA I	8.01	1.20
hCA II	6.13	0.038
hCA III	0.76	680
hCA IV	0.51	15.0
hCA VA	1.14	0.63
hCA VB	0.74	0.021
hCA VI	0.86	0.079
hCA VII	1.26	0.026
hCA IX	0.98	0.050
hCA XII	2.15	0.050
hCA XIII	0.69	0.023
hCA XIV	1.47	0.34

*Mean from three different determinations. Errors were in the range of ± 10% of the reported values.

Data of Table 1 show indeed GTX3 compound to be a CAI. For comparison reasons we also present the CA inhibition data of isoforms hCA I–hCA XIV with the sulfonamide CAI in clinical use dichlorophenamide (DCP). The inhibition profile of GTX3 is very particular, as the toxin shows a low micromolar inhibitory activity against the widespread, house-keeping isoforms hCA I and II (K_Is of 8.01 and 6.13 μM, respectively), whereas the remaining isoforms (hCA III-XIV) are inhibited more effectively, with K_Is in the range of 0.51–2.15 μM. The best inhibition was observed against the hCA IV (K_I of 0.51 μM), followed by the cytosolic isozyme hCA XIII (K_I of 0.69 μM). The remaining isoforms (hCA III, VA, VB, VI, VII, IX, XII and XIV) showed a rather compact behaviour, as the inhibition constant of GTX3 did not changed too much, being in the range of 0.74–2.15 μM. On the contrary, the sulphonamide inhibitor DCP is ineffective against CA III (K_I of 680 μM), has a micromolar activity against hCA I and IV (K_Is of 1.20–15.0 μM), and it is a nanomolar inhibitor of the other isoforms (hCA II, VA, VB and VI-XIV) against which the inhibition constants varies between 21 and 345 nM. It is well known that all sulfonamides investigated to date (as well as their isosteres, such as the sulfamates and sulfamides) coordinate to the Zn(II) ion from three CA active sites by means of the deprotonated sulfonamide nitrogen atom, making in addition a lot of other favourable interactions with amino acid residues from the enzyme active site[25–30]. Only recently we have discovered that coumarins[20] and lacosamide[31] bind in a different binding site, at the entrance of the cavity, being around 7 Å away from the metal ion. It should be mentioned that both sulfonamide isoform-selective CAIs as well as coumarin such derivatives, are in preclinical evaluations as antitumor/antimetastatic agents targeting hypoxic cancers[11,16,17].

As we were unable to obtain good crystals of GTX3 complexed to CAs, for X-ray crystallographic experiments, we performed molecular docking simulations of the molecule within the active sites of hCA I and II, in order to have a detailed insight regarding the inhibition mechanism of these natural compounds, which do not belong to well-known chemotypes inhibiting these enzymes[32–35]. The Induced-Fit docking (IFD) module which uses the Glide docking program to account for flexibility of the receptor has been used for docking under the Scrodinger

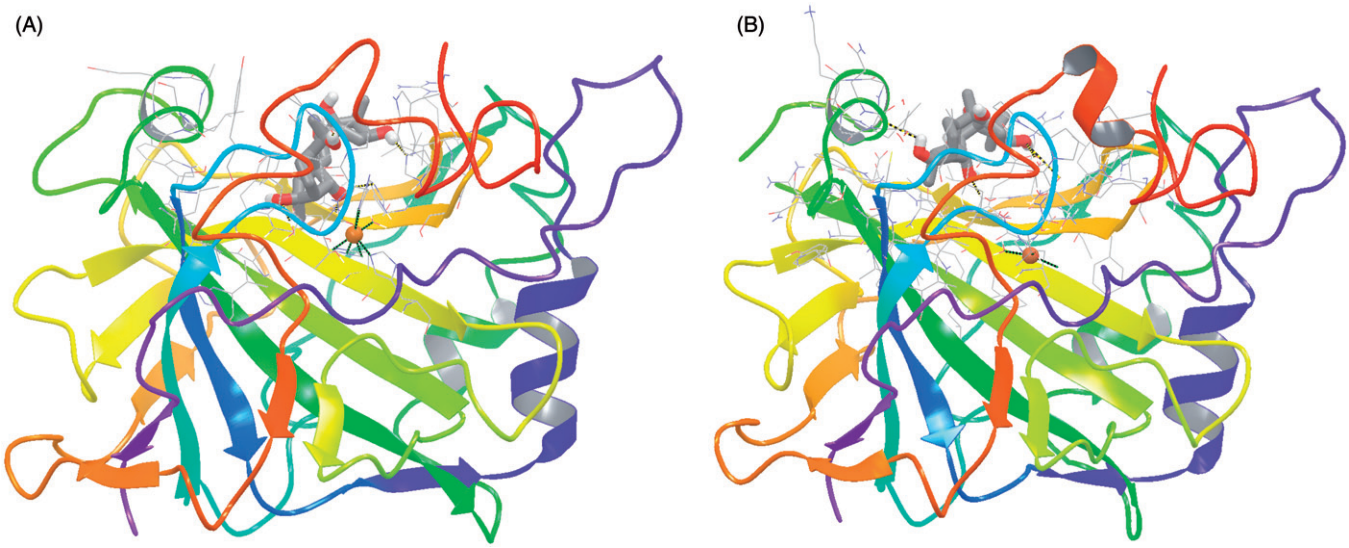

Figure 1. Binding of grayanotoxin III (GTX3) to hCA I (A) and hCA II (B). The protein backbone is represented with residue position default colors in Maestro, the catalytic Zn(II) ion as the pale brown sphere and GTX3 is shown as stick model (carbon gray, oxygen red, hydrogen white).

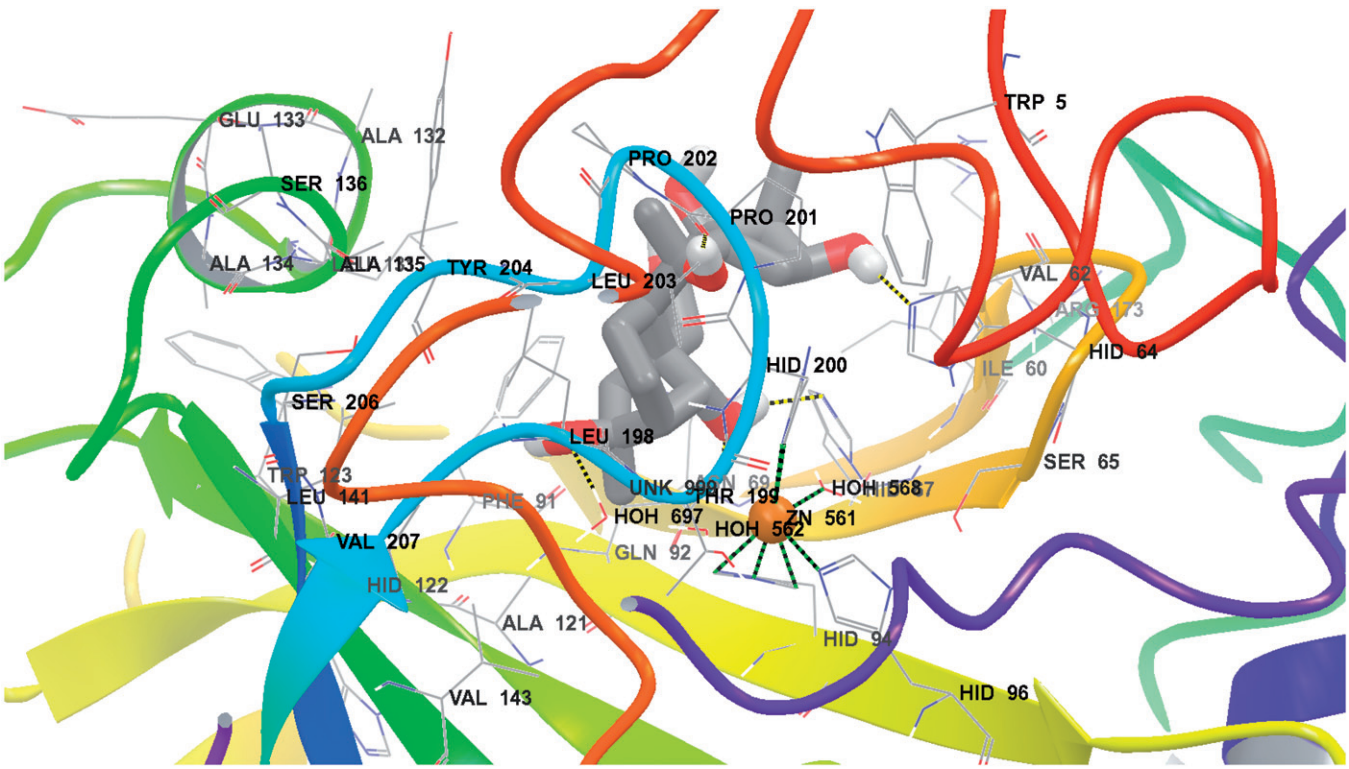

Figure 2. Detailed interactions of grayanotoxin III (GTX3) when bound to the hCA I active site. Docking score at hCA-I: −8.21 kcal/mol (Glide Induced Fit Docking). The protein backbone is represented with residue position default colors in Maestro, the catalytic Zn(II) ion as the pale brown sphere and GTX3 is shown as stick model (carbon gray, oxygen red, hydrogen white). Amino acid residues and water molecules involved in the interaction with grayanotoxin III are also evidenced (CPK colors; hCA I numbering system).

molecular modeling package[36–42]. Coordinate files of the two targets were available in PDB: file 2FW4[43] for hCA I docking and file[20] 3F8E for hCA II docking were employed.

As seen from Figures 1–3, the tetracyclic scaffold of grayanotoxin is easily accommodated within the active site of both CA isoforms used for the docking studies, hCA I and II. However, from the beginning we observed a notable difference in the location of the inhibitor molecule, which is buried deeply within the hCA I active site (Figure 1A) but found more towards the entrance of the cavity (Figure 1B) of hCA II. It is interesting to note that the active sites of these two CAs are very much similar except for the presence of a bulky His residue near the Zn(II) ion, His200 in hCA I, which in hCA II is Thr200[25,29,31,43]. As a consequence, the hCA I active site is tighter at the bottom of the cavity compared to hCA II, whereas towards the middle part and the entrance to the cavity they more or less have the same shape (although there are several amino acid residues which differ between these two cytosolic isoforms)[25,29,31,43]. The following close contacts between the inhibitor and the following amino acid residues of hCA I are observed (within 3 Å radial cavity of binding pocket amino acid residues from the inhibitor are listed here): His64, His67, His94, Gln92, Phe91, Ala121,

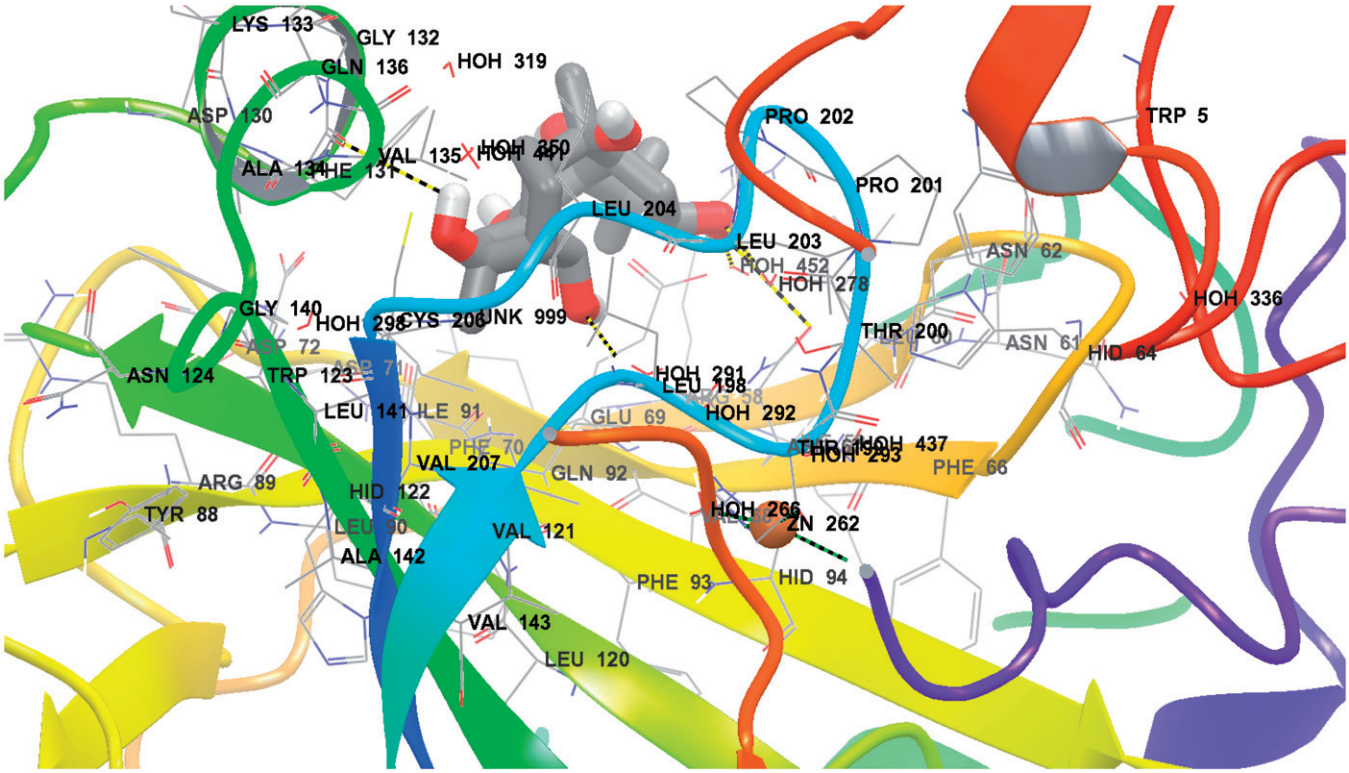

Figure 3. Detailed interactions of grayanotoxin III (GTX3) when bound to the hCA II active site. Docking score at CA-II: −8.29 kcal/mol; (Glide Induced Fit Docking). The protein backbone is represented with residue position default colors in Maestro, the catalytic Zn(II) ion as the pale brown sphere and GTX3 is shown as stick model (carbon gray, oxygen red, hydrogen white). Amino acid residues and water molecules involved in the interaction with grayanotoxin III are also evidenced (CPK colors; hCA I numbering system).

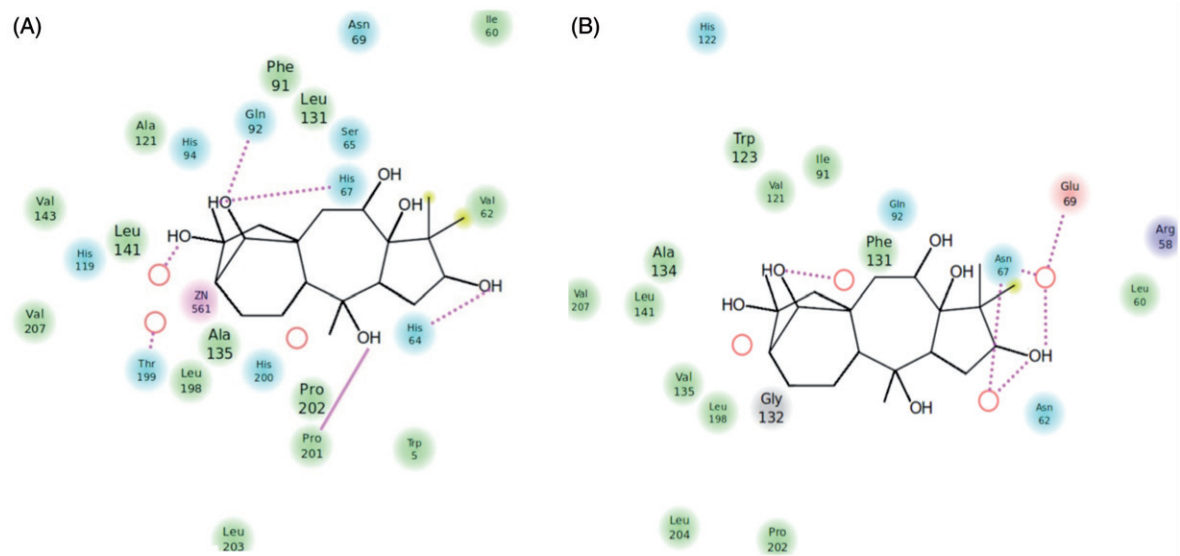

Figure 4. Ligand interaction diagrams for (A) hCA I and (B) hCA II. Residues are labeled and colored according to residue type (green, hydrophobic; cyan, polar; red, negative; purple, positive). Yellow markers on the ligand denote per-atom solvent accessible surface area and marker size shows the amount of exposure. Labeling of residue (font sizes) is used to represent the depth of a residue in the three dimensional view (i.e. ''closer'' to the viewer are shown in a large font, whereas, residues that are ''far away'' are shown with small font. While hydrogen bonds to side chains are represented with dashed, hydrogen bonds to backbones are represented as solid lines.

Val62, Leu198, His200, Pro201, Pro202 and Trp5. These amino acid residues were reported earlier to be involved in the binding of inhibitors/activators to the CA I active site (Figures 2 and 4)[25,29,31,43]. On the other hand, GTX3 was found in the coumarin-binding site of hCA II (Figures 3 and 4)[20], at around 8 Å away from the zinc ion. Obviously the inhibitor is not coordinated to the metal ion, but interacts by means of hydrogen bonds and van der Waals interactions with the following amino acid residues situated at the entrance of the cavity (within 3 Å radial cavity of binding pocket amino acid residues from the inhibitor are listed here): Asn67, Glu69, Gln92, Phe131, Val121, Ile91, Trp123, Leu141, Val135, Leu198 and Gly132. Three water molecules (HOH278, HOH291 and HOH452) form hydrogen bonds with the hydroxyl moieties found in the GTX3 molecule (Figures 3 and 4). This binding is very much similar to that of the *cis*-2-hydroxycinnamic acid derivative obtained by the in situ

hydrolysis of a coumarin natural product, identified as the first CAI belonging to this new class of inhibitors[20]. Also for that compound, many of the amino acid residues mentioned above, were observed to be involved in its binding in the enzyme-inhibitor adducts analyzed by means of high-resolution X-ray crystallography[20].

Docking scores are summarized in Table 2. Parallel to the experimental results, Glide XP score is slightly favourable for CA II (−8.29 kcal/mol) compared to CA II (−8.21 kcal/mol). IFD scores also showed same trend with Glide XP scores that CA II (−503.87 kcal/mol) is slightly more favorable than CA I (−494.58 kcal/mol).

In conclusion, we report here that grayanotoxin III is micromolar inhibitor (K_Is of 8.01–6.13 μM) of the widespread cytosolic isoforms CA I and II, and a submicromolar inhibitor (K_Is in the range of 0.51–2.15 μM) of the remaining cytosolic (CA III, VII and XIII), membrane-associated/transmembrane (CA IV, IX, XII and XIV), mitochondrial (CA VA and CA VB) and secreted (CA VI) isoforms. This inhibition profile is very different from that of the sulfonamide inhibitors, which have many clinical applications (antiglaucoma, diuretic, antiobesity, anticonvulsant or antitumor agents). The interesting inhibition profile, coupled with various possibilities of interacting with the enzyme active site make this natural compound an attractive lead for designing novel chemotypes acting as CAIs.

Among such botanical species which produce toxic nectar, all belonging to the Ericacee family, five are *Rododendrum. Rhododendron ponticum* subsp. *baeticum* is one of the most extensively cultivated rhododendrons in western Europe[44], and this and other related species became highly invasive over most Western Europe and New Zealand. They are on the other hand endemic in Turkey, in particular, *R. ponticum* and *R. flavum*, and populate the forests of the North of Anatolia. *Rhododendron ponticum* was introduced in 1763 in United Kingdom and thereafter widely diffused as invasive species[44]. The non controlled diffusion of *R. ponticum* is therefore a major concern for the public authorities in order to avoid the risk of alimentary contamination for the consumers and for the protection of the relevant economic sector of honey production[45]. Territory safeguard, biodiversity conservation, ecological function of the pollination, maintenance of the traditional and cultural heritage are only some of the issues connected with apiculture. In particular it represents one of the strategic sectors for the rural development in Turkey[45]. At the international level Turkey is at the second place for the number of bee colonies and at the third place for the production of honey, giving work to 240 000 people, with economic revenue of about 205 million dollars/year[45]. The need to control the expansion of *R. ponticum,* in addiction to be an internal problem, represents an emergency that Turkey has to face towards the international community as 95% of the produced honey is exported. A contamination of the honey would therefore produce, beside a relevant economical damage, a loss of image difficult to recovery at the international level[45].

Indeed mad honey may lead to severe intoxications, as shown in the introduction of this paper. Our study thus, may shed light regarding the biological activity of grayanotoxins present in this type of honey, for the inhibition of enzymes not normally associated with these toxins, but it also offers some interesting opportunities for the drug design of non-sulfonamide CAIs.

Experimental section

Chemistry. **GTX3** and **DCP** were from Sigma-Aldrich (Milan, Italy) whereas all CA isoforms were recombinant enzymes obtained in-house as reported earlier[20].

Table 2. Details of molecular docking results of GTX3 within the active sites of hCA I and hCA II using Induced Fit Docking (Glide/XP). Energy units are in kcal/mol.

	Glide_ Gscore	Glide_Lig_ efficiency In	Glide_ energy	Glide_ hbond	Glide_ lipo	Glide_ Ecoul	Glide_ Einter	Glide_ Evdw	Glide_Lig_ Efficiency	Glide_Lig_ eff_SA	Prime_ Coulomb	Prime_ Covalent	Prime_ VDW	Prime_ Sol_SA	Prime_ Sol_GB	Prime_ Energy	XP_ Hbond	IFD_ Score
hCA-1	−8.21	−1.93	−39.54	−0.91	−1.50	−13.81	0.91	−25.73	−0.32	−0.94	−8801.40	1346.85	−1325.02	59.50	−1007.33	−9727.40	−2.82	−494.58
hCA-2	−8.29	−1.94	−38.67	−0.51	−1.30	−13.23	0.89	−25.44	−0.32	−0.95	−8812.78	1342.83	−1401.30	96.11	−1132.16	−9911.30	−2.29	−503.87

CA inhibition. An Applied Photophysics stopped-flow instrument has been used for assaying the CA catalysed CO_2 hydration activity. Phenol red (at a concentration of 0.2 mM) has been used as indicator, working at the absorbance maximum of 557 nm, with 20 mM Hepes (pH 7.5) as buffer, and 20 mM Na_2SO_4 (for maintaining constant the ionic strength), following the initial rates of the CA-catalyzed CO_2 hydration reaction[24] for a period of 10–100 s. The CO_2 concentrations ranged from 1.7 to 17 mM for the determination of the kinetic parameters and inhibition constants. For each inhibitor at least six traces of the initial 5–10% of the reaction have been used for determining the initial velocity. The uncatalyzed rates were determined in the same manner and subtracted from the total observed rates. Stock solutions of inhibitor (0.1 mM) were prepared in distilled-deionized water and dilutions up to 0.01 nM were done thereafter with distilled-deionized water. Inhibitor and enzyme solutions were preincubated together for 15 min at room temperature prior to assay, in order to allow for the formation of the E-I complex (GTX3 was incubated also for longer periods, of 1–24 h, but no differences of activity have been detected). The inhibition constants were obtained by non-linear least-squares methods using PRISM 3, as reported earlier[16,17], and represent the mean from at least three different determinations. All CA isofoms were recombinant ones obtained in house as reported earlier[20,21].

Molecular docking studies. The IFD default protocol was used, consisting of: (i) Constrained minimization of the receptor with an RMSD cutoff of 0.18 Å. (ii) Initial Glide docking (SP) of each ligand using a soft potentials (0.5 van der Waals radii scaling of non-polar atoms of ligands and receptor using partial charge cutoff of 0.15). (iii) Derived docking poses were then refined using the Prime module of Schrodinger[36]. Residues within the 5.0 Å of ligand poses were minimized in order to form suitable conformations of poses at the active site of the receptor. (iv) Glide XP re-docking of each protein-ligand complex[36].

Declaration of interest

This research was financed by an FP7 EU project (Metoxia, to CTS) and the TAGEM-11/AR-GE/15.2011 project (to SK). The authors report no conflicts of interest. The authors alone are responsible for the content and writing of this article.

References

1. Chen SN, Zhang HP, Wang LQ, et al. Diterpenoids from the flowers of Rhododendron molle. J Nat Prod 2004;67:1903–6.
2. Terai T, Sato M, Narama I, et al. Transformation of grayanotoxin III to 10-epi-grayanotoxin III. Its X-ray crystallographic analysis and acute toxicity in mice. Chem Pharm Bull (Tokyo) 1996;44: 1245–7.
3. Koca I, Koca AF. Poisoning by mad honey: a brief review. Food Chem Toxicol 2007;45:1315–18.
4. Burke JW, Doskotch RW. High field 1H- and 13C-nmr assignments of grayanotoxins I, IV, and XIV isolated from Kalmia angustifolia. J Nat Prod 1990;53:131–7.
5. Akera T, Ku DD, Frank M, et al. Effects of grayanotoxin I on cardiac Na + K + -adenosine triphosphatase activity, transmembrane potential and myocardial contractile force. J Pharmacol Exp Ther 1976;199:247–54.
6. Sahin H, Aliyazicioglu R, Yildiz O, et al. Honey, pollen, and propolis extracts show potent inhibitory activity against the zinc metalloenzyme carbonic anhydrase. J Enzyme Inhib Med Chem 2011;26:440–4.
7. Supuran CT. Carbonic anhydrases: novel therapeutic applications for inhibitors and activators. Nat Rev Drug Discov 2008;7: 168–81.
8. Supuran CT. Carbonic anhydrase inhibitors. Bioorg Med Chem Lett 2010;20:3467–74.
9. Supuran CT. Bacterial carbonic anhydrases as drug targets: toward novel antibiotics? Front. Pharmacol 2011;2:1–6.
10. Pastorekova S, Parkkila S, Pastorek J, et al. Carbonic anhydrases: Current state of the art, therapeutic applications and future prospects. J Enzyme Inhib Med Chem 2004;19:199–229.
11. Neri D, Supuran CT. Interfering with pH regulation in tumours as a therapeutic strategy. Nature Reviews Drug Discovery 2011;10: 767–77.
12. Supuran CT, Scozzafava A, Casini A. Carbonic anhydrase inhibitors. Med Res Rev 2003;23:146–89.
13. Svastova E, Hulikova A, Rafajova M, et al. Hypoxia activates the capacity of tumor-associated carbonic anhydrase IX to acidify extracellular pH. Febs Lett 2004;577:439–45.
14. Ebbesen P, Pettersen EO, Gorr TA, et al. Taking advantage of tumor cell adaptations to hypoxia for developing new tumor markers and treatment strategies. J Enzyme Inhib Med Chem 2009;24:1–39.
15. Wykoff CC, Beasley NJ, Watson PH. Hypoxia-inducible expression of tumor-associated carbonic anhydrases. Cancer Res 2000;60: 7075–83.
16. Lou Y, McDonald PC, Oloumi A, et al. Targeting tumor hypoxia: suppression of breast tumor growth and metastasis by novel carbonic anhydrase IX inhibitors. Cancer Res 2011;71:3364–76.
17. Pacchiano F, Carta F, McDonald PC, et al. Ureido-substituted benzenesulfonamides potently inhibit carbonic anhydrase IX and show antimetastatic activity in a model of breast cancer metastasis. J Med Chem 2011;54:1896–902.
18. Supuran CT. Diuretics: From classical carbonic anhydrase inhibitors to novel applications of the sulfonamides. Curr Pharm Design 2008; 14:641–8.
19. De Simone G, Di Fiore A, Supuran CT. Are carbonic anhydrase inhibitors suitable for obtaining antiobesity drugs? Curr Pharm Design 2008;14:655–60.
20. Maresca A, Temperini C, Vu H, et al. Non-zinc mediated inhibition of carbonic anhydrases: coumarins are a new class of suicide inhibitors. J Am Chem Soc 2009;131:3057–62.
21. Carta F, Temperini C, Innocenti A, et al. Polyamines inhibit carbonic anhydrases by anchoring to the zinc-coordinated water molecule. J Med Chem 2010;53:5511–22.
22. Innocenti A, Vullo D, Scozzafava A, et al. Carbonic anhydrase inhibitors: interactions of phenols with the 12 catalytically active mammalian isoforms (CA I-XIV). Bioorg Med Chem Lett 2008;18: 1583–7.
23. Davis RA, Hofmann A, Osman A, et al. Natural product-based phenols as novel probes for mycobacterial and fungal carbonic anhydrases. J Med Chem 2011;54:1682–92.
24. Khalifah RG. The carbon dioxide hydration activity of carbonic anhydrase. I. Stop-flow kinetic studies on the native human isoenzymes B and C. The Journal of Biological Chemistry 1971; 246:2561–73.
25. Alterio V, Di Fiore A, D'Ambrosio K, et al. X-ray crystallography of CA inhibitors and its importance in drug design. In: Supuran CT, Winum JY, eds. Drug design of zinc-enzyme inhibitors: functional, structural, and disease applications. Hoboken (NJ): Wiley; 2009:73–138.
26. Alterio V, Di Fiore A, D'Ambrosio K, et al. Crystal structure of the catalytic domain of the tumor-associated human carbonic anhydrase IX. Proc Natl Acad Sci U S A 2009;106:16233–8.
27. Casini A, Antel J, Abbate F, et al. Carbonic anhydrase inhibitors: SAR and X-ray crystallographic study for the interaction of sugar sulfamates/sulfamides with isozymes I, II and IV. Bioorg Med Chem Lett 2003;13:841–5.
28. Avvaru BS, Wagner JM, Maresca A, et al. Carbonic anhydrase inhibitors. The X-ray crystal structure of human isoform II in adduct with an adamantyl analogue of acetazolamide resides in a less utilized binding pocket than most hydrophobic inhibitors. Bioorg Med Chem Lett 2010;20:4376–81.
29. Wagner J, Avvaru BS, Robbins AH, et al. Coumarinyl-substituted sulfonamides strongly inhibit several human carbonic anhydrase isoforms: solution and crystallographic investigations. Bioorg Med Chem 2010;18:4873–8.
30. Pacchiano F, Aggarwal M, Avvaru BS, et al. Selective hydrophobic pocket binding observed within the carbonic anhydrase II active site accommodate different 4-substituted-ureido-benzenesulfonamides and correlate to inhibitor potency. Chem Commun 2010;46: 8371–3.

31. Temperini C, Innocenti A, Scozzafava A, et al. The coumarin-binding site in carbonic anhydrase accommodates structurally diverse inhibitors: the antiepileptic lacosamide as an example and lead molecule for novel classes of carbonic anhydrase inhibitors. J Med Chem 2010;53:850–4.
32. Durdagi S, Senturk M, Ekinci D, et al. Kinetic and docking studies of phenol-based inhibitors of carbonic anhydrase isoforms I, II, IX and XII: evidence of a new binding mode within the enzyme active site. Bioorg Med Chem 2011;19:1381–9.
33. Balaydin H, Turker H, Durdagi S, et al. Inhibition of human carbonic anhydrase isozymes I, II, and VI with a series of bisphenol, methoxy and bromophenol compounds. J Enzy Inh Med Chem 2012;27:467–75.
34. Innocenti A, Durdagi S, Doostdar N, et al. Nanoscale enzyme inhibitors: fullerenes inhibit carbonic anhydrase by occluding the active site entrance. Bioorg Med Chem 2010;18: 2822–8.
35. Talaz O, Cavdar H, Durdagi S, et al. Synthesis of 1,4-bis(indolin-1-ylmethyl)benzene derivatives and their structure-activity relationships for the interaction of human carbonic anhydrase isoforms I and II. Bioorg Med Chem 2013;21:1477–82.
36. Friesner RA, Murphy RB, Repasky Frye LL, et al. Extra precision glide: docking and scoring incorporating a model of hydrophobic enclosure for protein-ligand complexes. J Med Chem 2006;49: 6177–96.
37. Subbotina J, Yarov-Yarovoy V, Lees-Miller J, et al. Structural refinement of the hERG1 pore and voltage-sensing domains with ROSETTA-membrane de-novo modeling and molecular-dynamics simulations. Proteins: Struct Funct Bioinform 2010;78:2922–34.
38. Cakmak R, Durdagi S, Ekinci D, et al. Design, synthesis and biological evaluation of novel nitroaromatic compounds as potent glutathione reductase inhibitors. Bioorg Med Chem Lett 2011;21:5398–402.
39. Politi A, Durdagi S, Moutevelis-Minakakis P, et al. Development of accurate binding affinity predictions of novel renin inhibitors through molecular docking studies. J Mol Graph Model 2010; 29:425–35.
40. Durdagi S, Zhao C, Cuervo JE, Noskov SY. Atomistic models for free energy evaluation of drug binding to membrane proteins. Curr Med Chem 2011;18:2601–11.
41. Mavromoustakos T, Durdagi S, Koukoulitsa C, et al. Strategies in the rational drug design. Curr Med Chem 2011;18:2517–30.
42. Durdagi S, Subbotina J, Lees-Miller J, et al. Insights into molecular mechanism of herg1 channel activation and blockade by drugs. Curr Med Chem 17: 3514–32.
43. Temperini C, Scozzafava A, Supuran CT. Carbonic anhydrase activators: the first X-ray crystallographic study of an adduct of isoform I. Bioorg Med Chem Lett 2006;16:5152–56.
44. Milne RI, Abbott RJ. Origin and evolution of invasive naturalized material of *Rhododendron ponticum* L. in the British Isles. Mol Ecol 2000;9:541–56.
45. Food and Agriculture Organization of the United Nations. Data available at: http://faostat.fao.org/site/339/default.aspx [last accessed 22 Jul 2013].